PROCEEDINGS OF THE INTERNATIONAL CONFERENCE ON
NUMERICAL ANALYSIS AND APPROXIMATION THEORY
NAAT2006, CLUJ-NAPOCA (ROMANIA), JULY 5–8, 2006, pp. 1–14

HIGH ORDER WENO FINITE VOLUME SCHEMES USING POLYHARMONIC SPLINE RECONSTRUCTION

TERHEMEN ABOIYAR, EMMANUIL H. GEORGOULIS, AND ARMIN ISKE

Abstract. Polyharmonic splines are utilized in the WENO reconstruction of finite volume discretizations, yielding a numerical method for scalar conservation laws of arbitrary high order. The resulting WENO reconstruction method is, unlike previous WENO schemes using polynomial reconstructions, numerically stable and very flexible. Moreover, due to the theory of polyharmonic splines, optimal reconstructions are obtained in associated native Sobolev-type spaces, called Beppo Levi spaces. This in turn yields a very natural choice for the oscillation indicator, as required in the WENO reconstruction method. The key ingredients of the proposed polyharmonic spline WENO reconstruction algorithm are explained in detail, and one numerical example is given for illustration.

1. Introduction

The modelling of many physical problems leads to time-dependent conservation laws. Finite volume (FV) schemes are popular conservative numerical methods for solving hyperbolic conservation laws, where classical FV methods are typically of low order. During the last decade, high order FV schemes were developed in combination with *shock capturing* or *front tracking* techniques in order to treat sharp gradients or discontinuities of the solution, *shocks*, while providing high order convergence rates. Among such powerful FV discretizations are ENO and WENO reconstructions in combination with either TVD-like Runge-Kutta methods [22] or with the more recent high order flux evaluation by using ADER methods [29]. For a comprehensive treatment of finite volume methods for hyperbolic conservation problems, see [16], for their applications in fluid dynamics, see [30].

Essentially non-oscillatory (ENO) and *weighted essentially non-oscillatory* (WENO) reconstructions are used in combination with appropriate time step discretizations to obtain conservative high order finite volume

Key words and phrases. finite volume methods, WENO reconstruction, hyperbolic conservation laws, polyharmonic splines.

methods for hyperbolic conservation laws. First ENO reconstructions for one-dimensional conservation problems were developed by Harten, Engquist, Osher & Chakravarthy [9] in 1987. Somewhat later, ENO methods on two-dimensional structured meshes were proposed by Abgrall [1], Harten & Chakravarthy [8], and Sonar [25].

The basic idea behind ENO schemes is to first select, for each cell of the finite volume discretization, a set of stencils, each comprising a set of neighbouring cells. Then, for each stencil, a recovery polynomial is computed, which interpolates given cell averages over the cells in the stencil. Amongst the different recovery polynomials, one for each stencil, the *smoothest* (i.e., least oscillatory) is selected, where the smoothness of the polynomial reconstruction is measured by using a suitable *oscillation indicator*. ENO schemes yield high order finite volume methods, provided that high order polynomial reconstructions are utilized. Moreover, spurious oscillations of the solution can be avoided.

Later in 1994, WENO schemes were developed to improve ENO schemes. First WENO schemes for one-dimensional conservation problems date back to Liu, Osher & Chan [17] and to Jiang & Shu [14], and were later extended to the two-dimensional case by Friedrich [7] and Hu & Shu [10]. In the WENO framework, the whole set of stencils and their corresponding polynomial reconstructions are used to construct a *weighted* sum of reconstruction polynomials to approximate the solution over a *control volume* of the finite volume method. The required weights are determined by using the above mentioned oscillation indicator of the ENO scheme.

As observed in numerical experiments [1], ENO and WENO schemes using *polynomial* reconstruction may lead to severe numerical instabilities. Although several alternative reconstruction schemes were proposed [1, 2, 7, 11, 24, 26, 28], both the lack of numerical stability and the high computational complexity are still critical points for WENO reconstruction schemes, especially for unstructured meshes.

This paper proposes WENO reconstructions over conforming unstructured triangulations by using *polyharmonic splines* rather than polynomials. Polyharmonic splines yield numerically stable reconstruction schemes, which are based on radial basis functions, being traditional and powerful tools from multivariate scattered data approximation. WENO reconstruction by polyharmonic splines is, in comparison with polynomial reconstruction not only more stable, but also more flexible. Moreover, polyharmonic splines yield optimal reconstructions (in the sense of Micchelli and Rivlin [19]) in their associated native Sobolev-type spaces, called *Beppo Levi spaces*. The semi-norm of the Beppo Levi spaces gives rise to a natural choice for the required oscillation indicator. More details on these and

other important features of polyharmonic splines are explained in Section 3. Further properties of polyharmonic splines, especially concerning WENO reconstruction, are discussed in Section 4. Supporting numerical examples are finally provided in Section 5. But let us first provide a short discussion on the finite volume method.

2. Finite Volume Formulation

We consider solving the two dimensional scalar conservation law

$$\frac{\partial u}{\partial t} + \nabla \cdot F(u) = 0 \tag{1}$$

numerically by using standard finite volume discretization on a computational domain $\Omega \subset \mathbb{R}^2$ with polygonal boundary and for compact time interval $I \subset \mathbb{R}$, subject to appropriate initial and boundary conditions. The solution $u : I \times \Omega \to \mathbb{R}^2$ of (1) denotes the density (or concentration) of a physical quantity being subject to a conservation law. Moreover, $F(u) = (f_1(u), f_2(u))^T$ in (1) denotes the flux function, which we assume to be sufficiently smooth. It is well known that for nonlinear flux F the solution u of (1) may spontaneously develop discontinuities in finite time, even at smooth input data (i.e., for smooth initial and boundary conditions and smooth domain boundaries).

For the solution of (1) we consider using the finite volume method on unstructured triangulations. In this classical discretization scheme, the computational domain Ω is partitioned through a triangulation $\mathcal{T} = \{T\}_{T\in\mathcal{T}}$ containing finitely many closed triangles with disjoint interior and whose union is Ω. Moreover, the intersection of two distinct triangles in $\mathcal{T}$ may either be empty, or an edge in $\mathcal{T}$, or a vertex in $\mathcal{T}$. The latter states that $\mathcal{T}$ is a *conforming* triangulation of Ω.

For any triangle $T \in \mathcal{T}$, the semi-discrete scheme, based on the integral form of (1), has the form

$$\frac{d}{dt}\bar{u}_T + \frac{1}{|T|}\int_{\partial T} F \cdot \mathbf{n}\, ds = 0, \qquad \text{for } T \in \mathcal{T}, \tag{2}$$

where

$$\bar{u}_T \equiv \bar{u}_T(t) = \frac{1}{|T|}\int_T u(t,x)\, dx, \qquad \text{for } T \in \mathcal{T}, t \in I,$$

denotes the *cell average* of u over triangle $T \in \mathcal{T}$ at time $t \in I$. Moreover, $\mathbf{n}$ in (2) is the outward unit normal vector of the triangle's boundary ∂T and $|T|$ is the area of triangle T.

2.1. **Spatial Discretization.** The boundary ∂T of triangle $T \in \mathcal{T}$ is given by the union of three edges, say $\Gamma_1, \Gamma_2, \Gamma_3$, in the triangulation $\mathcal{T}$, i.e.,

$$\partial T = \bigcup_{j=1}^{3} \Gamma_j,$$

so that the line integral in (2) can be represented as

$$\int_{\partial T} F \cdot \mathbf{n}\, ds = \sum_{j=1}^{3} \int_{\Gamma_j} F(u(t,s)) \cdot \mathbf{n}_j\, ds, \tag{3}$$

where $\mathbf{n}_j$ is the outward unit normal vector for edge Γ_j. We discretize the integral on the right hand side of (3) by using a q-point Gaussian integration formula, for some specific $q \in \mathbb{N}$ which determines the order of the resulting quadrature rule.

Now let $G_1, \ldots, G_q$ and $w_1, \ldots, w_q$ denote the Gaussian points and weights for the triangle's edge Γ_j. Then, the Gaussian quadrature formula

$$\int_{\Gamma_j} F(u(t,s)) \cdot \mathbf{n}_j\, ds \approx |\Gamma_j| \sum_{\ell=1}^{q} w_\ell F(u(t,G_\ell)) \cdot \mathbf{n}_j, \qquad j = 1,2,3,$$

yields high order approximation to the line integral (3), and so (2) becomes

$$\frac{d}{dt}\bar{u}_T(t) + \frac{1}{|T|} \sum_{j=1}^{3} |\Gamma_j| \sum_{\ell=1}^{q} w_\ell F(u(t,G_\ell)) \cdot \mathbf{n}_j = 0.$$

Finally, we replace the terms $F(u(t,G_\ell)) \cdot \mathbf{n}_j$, $1 \le \ell \le q$, by a *numerical flux function* to approximate the flux across the boundary of neighbouring triangles to $T \in \mathcal{T}$. In our implementation, we decided to work with the *Lax-Friedrichs flux*, given by

$$\begin{aligned} &F(u(t,G_\ell)) \cdot \mathbf{n} \approx \tilde{F}(u(t,G_\ell)) \cdot \mathbf{n} = \\ &\frac{1}{2}\left[(F(u_{\text{in}}(t,G_\ell)) + F(u_{\text{out}}(t,G_\ell))) \cdot \mathbf{n} - \sigma(u_{\text{in}}(t,G_\ell) - u_{\text{out}}(t,G_\ell)) \right], \end{aligned} \tag{4}$$

where σ is an upper bound for the eigenvalues of the flux function's Jacobian matrix in the normal direction $\mathbf{n}$. Moreover, for time $t \in I$, $u_{\text{in}}(t,G_\ell)$ in (4) is the function value of the solution's representation over triangle T, and $u_{\text{out}}(t,G_\ell)$ is the function value of the corresponding representation over the neighbouring triangle that shares the edge Γ_j with T.

According to the finite volume discretization (see [16]), approximations to the spatial cell averages $\bar{u}_T$ are at any time step given by a one-step

update of the form

$$L_T(\bar{u}_T(t)) = -\frac{1}{|T|}\sum_{j=1}^{3}|\Gamma_j|\sum_{\ell=1}^{q} w_\ell \tilde{F}(u(t,G_\ell))\cdot \mathbf{n}_j,$$

for some specific univariate function L_T, see (5).

To this end, the spatial integration requires a suitable reconstruction from the current cell averages $\{\bar{u}_T\}_{T\in\mathcal{T}}$, where traditional reconstruction methods are based on polynomial interpolation. Especially in combination with unstructured meshes, however, polynomial reconstruction schemes often suffer from their lack of flexibility. Moreover, polynomial reconstructions may lead to severe numerical instabilities [1]. Our preferred reconstruction method is based on interpolation by polyharmonic splines, as further discussed in Sections 3 and 4.

2.2. **Time Discretization.** When it comes to numerical flux evaluation, commonly used approximations methods rely on a set of ordinary differential equations (ODEs) of the form

$$\frac{d}{dt}\bar{u}_T(t) = L_T(\bar{u}_T(t)), \qquad \text{for } T\in\mathcal{T}, \tag{5}$$

where each $L_T:\mathbb{R}\to\mathbb{R}$, $T\in\mathcal{T}$, is a univariate function. The system (5) of ODEs is solved by using a suitable *total variation diminishing* (TVD) Runge-Kutta (RK) method, which was first introduced by Shu & Osher [23].

Here we use for any $T\in\mathcal{T}$ the third order TVD-RK method,

$$\begin{aligned}
\bar{u}_T^{(1)} &= \bar{u}_T^n + \tau L_T(\bar{u}_T^n),\\
\bar{u}_T^{(2)} &= \frac{3}{4}\bar{u}_T^n + \frac{1}{4}\bar{u}_T^{(1)} + \frac{1}{4}\tau L_T(\bar{u}_T^{(1)}),\\
\bar{u}_T^{n+1} &= \frac{1}{3}\bar{u}_T^n + \frac{2}{3}\bar{u}_T^{(2)} + \frac{2}{3}\tau L_T(\bar{u}_T^{(2)}),
\end{aligned} \tag{6}$$

where τ denotes the time step. Further details are immaterial for the purposes of this paper. Therefore, we refer the interested reader to [23].

3. Polyharmonic Spline Reconstruction from Cell Averages

Let us first discuss the more general radial basis function method, before we turn to the special case of reconstruction by polyharmonic splines.

3.1. **Reconstruction by Radial Basis Functions.** Given a conforming triangulation $\mathcal{T}=\{T\}_{T\in\mathcal{T}}$ and a triangle $T\in\mathcal{T}$, consider a *stencil*

$$\mathcal{S} = \{T_1, T_2, \ldots, T_n\} \subset \mathcal{T}$$

of size $\#\mathcal{S} = n$, containing T, i.e., $T \subset \mathcal{S}$. Suppose the triangles in stencil $\mathcal{S}$ are associated with linearly independent functionals $\{\lambda_T\}_{T\in\mathcal{S}}$,

$$\lambda_T(u) = \frac{1}{|T|}\int_T u(x)\,dx, \qquad \text{for } T \in \mathcal{T} \text{ and } u(x) \equiv u(t,x),$$

where for any $T \in \mathcal{T}$ the linear functional λ_T is referred to as the *cell average operator* for triangle T.

Now on given cell averages $\{\lambda_T(u)\}_{T\in\mathcal{S}}$ for any stencil $\mathcal{S} \subset \mathcal{T}$, we consider solving the reconstruction problem $u\big|_{\mathcal{S}} = s\big|_{\mathcal{S}}$, i.e.,

$$\lambda_T(u) = \lambda_T(s), \qquad \text{for all } T \in \mathcal{S}, \tag{7}$$

with assuming

$$s(x) = \sum_{T\in\mathcal{S}} c_T \lambda_T^y \phi(\|x-y\|) + p(x), \qquad p \in \mathcal{P}_k^d, \tag{8}$$

for the form of the reconstruction s, where $\phi : [0,\infty) \to \mathbb{R}$ is a fixed *radial basis function*, where $\|\cdot\|$ is the Euclidean norm on $\mathbb{R}^d$, and where $\mathcal{P}_k^d$ is the linear space of all d-variate polynomials of order at most k (i.e., of degree at most $k-1$). Recall that the dimension of $\mathcal{P}_k^d$ is $q = \dim(\mathcal{P}_k^d) = \binom{k-1+d}{d}$. Moreover, λ_T^y in (8) denotes the action of the linear functional λ_T w.r.t. variable y, i.e.,

$$\lambda_T^y \phi(\|x-y\|) = \frac{1}{|T|}\int_T \phi(\|x-y\|)\,dy.$$

The order k of $p \in \mathcal{P}_k^d$ is given by the order $k \equiv k(\phi)$ of the radial basis function ϕ. Possible choices for ϕ are, along with their order k, shown in Table 1. For further details on radial basis function, we refer to the recent textbooks [5, 13, 27].

TABLE 1. Radial basis functions (RBFs) and their orders.

RBF	$\phi(r)$	**Parameters**	**Order**
Polyharmonic Splines	r^{2k-d} for d odd $r^{2k-d}\log(r)$ for d even	$k \in \mathbb{N},\ k > d/2$ $k \in \mathbb{N},\ k > d/2$	k k
Gaussians	$\exp(-r^2)$		0
Multiquadrics	$(1+r^2)^\nu$	$\nu > 0, \nu \notin \mathbb{N}$	$\lceil \nu \rceil$
Inverse Multiquadrics	$(1+r^2)^\nu$	$\nu < 0$	0

Note that the reconstruction s in (8) contains $n+q$ parameters, n for its major part and q for its polynomial part, but at only $n = \#\mathcal{S}$ interpolation conditions in (7). To eliminate the additional q degrees of freedom, we consider solving (7) under linear constraints

$$\sum_{T\in\mathcal{S}} c_T \lambda_T(p) = 0, \qquad \text{for all } p \in \mathcal{P}_k^d, \tag{9}$$

where λ_T is the cell average operator of triangle T. This leads us to the $(n+q)\times(n+q)$ linear system

$$\begin{bmatrix} A & P \\ P^T & 0 \end{bmatrix} \begin{bmatrix} c \\ d \end{bmatrix} = \begin{bmatrix} u\big|_{\mathcal{S}} \\ 0 \end{bmatrix}, \tag{10}$$

where

$$A = (\lambda_T^x \lambda_R^y \phi(\|x-y\|))_{T,R\in\mathcal{S}} \in \mathbb{R}^{n\times n} \text{ and } P = (\lambda_T(x^\alpha))_{T\in\mathcal{S},0\le|\alpha|<k} \in \mathbb{R}^{n\times q},$$

and $u\big|_{\mathcal{S}} = (\lambda_T(u))_{T\in\mathcal{S}} \in \mathbb{R}^n$.

The linear system (10) has for any radial basis function ϕ in Table 1 a unique solution for the unknown coefficients $c \in \mathbb{R}^n$ (for the major part of s) and $d \in \mathbb{R}^q$ (for the polynomial part of s), provided that the set $\{\lambda_T\}_{T\in\mathcal{S}}$ of cell average operators is $\mathcal{P}_k^d$-*unisolvent*, i.e., for $p \in \mathcal{P}_k^d$ we have

$$\lambda_T(p) = 0 \quad \text{for all } T \in \mathcal{T} \qquad \Longrightarrow \qquad p \equiv 0,$$

in which case any polynomial from $\mathcal{P}_k^d$ can uniquely be reconstructed from its values $\{\lambda_T(p)\}_{T\in\mathcal{S}}$. This standard result dates back to the seminal work of Micchelli [18].

3.2. **Reconstruction by Polyharmonic Splines.** Now let us turn to polyharmonic splines, whose reconstruction scheme is due to the groundbreaking work of Duchon [6]. Polyharmonic splines are our preferred choice for ϕ when solving (7),(9). This particular choice is justified by several relevant reasons, as it will become obvious in the ensuing discussion of this paper.

In the polyharmonic spline reconstruction method, the radial basis function $\phi \equiv \phi_{d,k} : [0,\infty) \to \mathbb{R}$ in (8) is, for $d, k \in \mathbb{N}$ with $2k > d$, given by

$$\phi_{d,k}(r) = \begin{cases} r^{2k-d} & \text{for } d \text{ odd;} \\ r^{2k-d}\log(r) & \text{for } d \text{ even;} \end{cases}$$

where d denotes the space dimension and k is the order of the basis function $\phi_{d,k}$, see Table 1. Note that the function $\phi_{d,k}$ is a fundamental solution of the k-th iterated Laplacian, i.e.,

$$\Delta^k \phi_{d,k}(\|x\|) = C \cdot \delta_x,$$

for some specific constant C and where δ_x denotes the usual Dirac point evaluation functional at $x \in \mathbb{R}^d$.

To make one important example, the special case $d = k = 2$ leads us to the popular *thin plate spline* $\phi_{2,2}(r) = r^2 \log(r)$, which is a fundamental solution of the biharmonic equation on $\mathbb{R}^2$. In this case, the reconstruction s in (8) has the form

$$s(x) = \sum_{T \in \mathcal{S}} c_T \lambda_T^y \left(\|x - y\|^2 \log(\|x - y\|) \right) + d_1 + d_2 \xi + d_3 \eta,$$

where we let ξ and η denote the two coordinates of $x = (\xi, \eta)^T \in \mathbb{R}^2$.

3.3. **Optimal Reconstruction in Beppo Levi Spaces.** One important feature of the polyharmonic spline method, with using $\phi_{d,k}$, is their optimal reconstruction property in the *Beppo Levi space*

$$\mathrm{BL}^k(\mathbb{R}^d) = \{u : D^\alpha u \in L^2(\mathbb{R}^d) \text{ for all } |\alpha| = k\} \subset C(\mathbb{R}^d),$$

being equipped with the semi-norm

$$|u|_{\mathrm{BL}^k(\mathbb{R}^d)} = \sum_{|\alpha|=k} \binom{k}{\alpha} \|D^\alpha u\|^2_{L^2(\mathbb{R}^d)}.$$

This variational property, due to Duchon [6], says that for $\phi \equiv \phi_{d,k}$ the reconstruction $s \in \mathrm{BL}^k(\mathbb{R}^d)$ in (8) minimizes the energy $|\cdot|_{\mathrm{BL}^k(\mathbb{R}^d)}$ among all elements in $\mathrm{BL}^k(\mathbb{R}^d)$ satisfying (7). This implies that for any $u \in \mathrm{BL}^k(\mathbb{R}^d)$, we have

$$|s|_{\mathrm{BL}^k(\mathbb{R}^d)} \leq |u|_{\mathrm{BL}^k(\mathbb{R}^d)}, \qquad \text{with } u\big|_{\mathcal{S}} = s\big|_{\mathcal{S}}, \tag{11}$$

where $s \in \mathrm{BL}^k(\mathbb{R}^d)$ is the reconstruction of u from data $\{\lambda_T(u)\}_{T \in \mathcal{S}}$, i.e., s satisfies (7).

For thin plate splines, where $d = k = 2$, the semi-norm $|\cdot|_{\mathrm{BL}^2(\mathbb{R}^2)}$ of the corresponding Beppo Levi space $\mathrm{BL}^2(\mathbb{R}^2)$ is for any $u \in \mathrm{BL}^2(\mathbb{R}^2)$ given by the bending energy

$$|u|^2_{\mathrm{BL}^2(\mathbb{R}^2)} = \int_{\mathbb{R}^2} \left[\left(\frac{\partial^2 u}{\partial \xi^2} \right)^2 + 2 \left(\frac{\partial^2 u}{\partial \xi \partial \eta} \right)^2 + \left(\frac{\partial^2 u}{\partial \eta^2} \right)^2 \right] d\xi \, d\eta$$

of a thin plate of infinite extent, which explains the naming "thin plate spline" for the minimizer s in (11) .

3.4. **Numerical Stability and Arbitrary Approximation Order.** As shown in our previous paper [12], the implementation of the polyharmonic spline reconstruction scheme requires particular care, especially for the sake of numerical stability. This is mainly because a direct solution of (7), (9) may lead to coefficient matrices in (10), whose spectral condition number is very large in situations where the barycenters of two distinct triangles in stencil $\mathcal{S} \subset \mathcal{T}$ are very close. This important observation, due to Narcowich & Ward [20] has motivated the construction of a preconditioner for the linear system (10) in [12]. The bottom line message of [12] is that there is a stable solution for solving (7),(9), whenever the reconstruction problem is well-conditioned. A concrete choice for a very simple and effective preconditioner is proposed in [12]. In summary, polyharmonic splines are, in combination with the preconditioner in [12] stable methods for solving (7),(9), unlike any other radial basis function in Table 1.

Furthermore, it is shown in [12] that the *local approximation order* of the polyharmonic spline reconstruction method is arbitrarily high. More precisely, when working with $\phi \equiv \phi_{d,k}$ the local approximation order is k, and so the *smoothness parameter* k in $\phi_{d,k}$ can be used to obtain a desired target approximation order k. For further details, we refer to [12].

4. Features of Polyharmonic Spline WENO Reconstruction

To explain further important features and advantages of polyharmonic spline reconstruction, let us first briefly recall the general form of the WENO reconstruction scheme.

Algorithm 1. (WENO Reconstruction)

Input: *triangle* $T \in \mathcal{T}$*, stencils* $\mathcal{S} = \{\mathcal{S}_i\}_i$ *satisfying* $T \subset \mathcal{S}_i \subset \mathcal{T}$ *for all* i*.*

(1) FOR *each stencil* $\mathcal{S}_i$ **DO**

(1a) *Compute reconstruction* s_i *from* $\{\lambda_T(u)\}_{T\in\mathcal{S}_i}$ *satisfying* $s\big|_{\mathcal{S}_i} = u\big|_{\mathcal{S}_i}$*;*
(1b) *Compute oscillation* $\mathcal{I}(s_i)$ *of* s_i *according to oscillation indicator* $\mathcal{I}$*;*

(2) *Compute non-negative weights* ω_i *satisfying* $\sum_i \omega_i = 1$ *from values* $\mathcal{I}(s_i)$*.*

Output: *WENO reconstruction*

$$s(x) = \sum_i \omega_i s_i(x). \tag{12}$$

4.1. **Enhanced Flexibility in Stencil Selection.** Note that the solution of (10) consists of $n + q$ conditions, where we merely require $n \geq q$ for the well-posedness of the reconstruction problem (8),(9). But otherwise, there is *no* further restriction on the number $n = \#\mathcal{S}$ of given data $\{\lambda_T(u)\}_{T\in\mathcal{S}}$.

This makes up a main difference to polynomial reconstruction, where we require $n = q$, in which case the number of given data (i.e., number of cell averages) is for *any* individual stencil dictated by the chosen degree of the polynomial space. In fact, this severe restriction is considered as a major drawback of the polynomial reconstruction scheme. In contrast, the polyharmonic spline reconstruction scheme is much less restrictive, when it comes to the selection of the individual stencils and their sizes. Indeed, the additional freedom allows for more flexible construction strategies for the stencil selection.

4.2. **Natural Oscillation Indicator.** According to the WENO reconstruction scheme, Algorithm 1, we need to work with an oscillation indicator $\mathcal{I}$ which measures for any stencil $\mathcal{S}_i$ the *smoothness* of the corresponding reconstruction s_i. To this end, recall that the *Beppo Levi spaces* $\mathrm{BL}^k(\mathbb{R}^d)$ are the optimal recovery spaces for polyharmonic splines (see Subsection 3.3), which gives rise to define the oscillation indicator $\mathcal{I}$ as

$$\mathcal{I}(s) = |s|^2_{\mathrm{BL}^k(\mathbb{R}^d)}, \qquad \text{for } s \in \mathrm{BL}^k(\mathbb{R}^d).$$

For each triangle $T \in \mathcal{T}$ we use the oscillation indicator $\mathcal{I}$ to compute for any polyharmonic spline reconstruction s_i its corresponding weight ω_i. To this end, we first compute intermediate values

$$\gamma_i = \frac{1}{(\epsilon + \mathcal{I}(s_i))^\rho} \qquad \text{for some } \epsilon, \rho > 0. \tag{13}$$

The non-negative weights for the polyharmonic spline WENO reconstruction s in (12) are then for any i given by $\omega_i = \gamma_i / \sum_j \gamma_j$. Note that the weights ω_i form a partition of unity, i.e., $\sum_i \omega_i = 1$.

For any reference triangle $T \in \mathcal{T}$, the resulting approximation $s \equiv s_T$ to u over T is used to replace u in the numerical flux (4), where in particular u_{in} is replaced by s_{in} and u_{out} is replaced by s_{out}.

The basic idea of the WENO reconstruction method is that for stencils $\mathcal{S}_i$ lying in regions around triangle T, where the solution u is *smooth*, the corresponding weights ω_i should be large. In contrast, for stencils $\mathcal{S}_i$ in regions where the solution u is subject to strong variation (e.g. due to sharp gradients or discontinuities), the corresponding weights ω_i should be close to zero. In this case, the resulting WENO reconstruction s in (12) is essentially non-oscillatory by construction, as desired.

5. Numerical Results

We consider solving the two-dimensional linear advection equation

$$u_t + u_\xi + u_\eta = 0, \qquad \text{for } u \equiv u(t,x) \text{ with } x = (\xi, \eta) \in \mathbb{R}^2, \tag{14}$$

in combination with the initial condition

$$u_0(x) = u(0,x) = \sin(2\pi(\xi+\eta)), \qquad \text{for } x \in \Omega, \tag{15}$$

on the computational domain $\Omega = [-0.5, 0.5] \times [-0.5, 0.5] \subset \mathbb{R}^2$, $d = 2$, by using the proposed finite volume method of this paper. We decided to take this particular numerical example from our previous paper [15]. This is mainly for the purpose of comparison with the finite volume method in [15], where polynomials are used in the WENO reconstruction.

In the WENO reconstruction, Algorithm 1, we work with thin plate splines, $k = 2$. Moreover, we let $I = [0, 1]$ for the time interval and we use periodic boundary conditions, so that the reference solution $\tilde{u}(1, x)$ coincides at final time $t = 1$ with the initial condition u_0 in (15), so that $u_0(x) \equiv \tilde{u}(1, x)$.

The numerical experiments are performed by using a sequence $\mathbf{A}_1$–$\mathbf{A}_3$ of three *mildly distorted* triangular meshes of decreasing mesh width $h = 1/16, 1/32, 1/64$. We denote the obtained numerical solution of (14),(15) by u_h. The triangulations $\mathbf{A}_1$–$\mathbf{A}_3$ are shown in Figure 1.

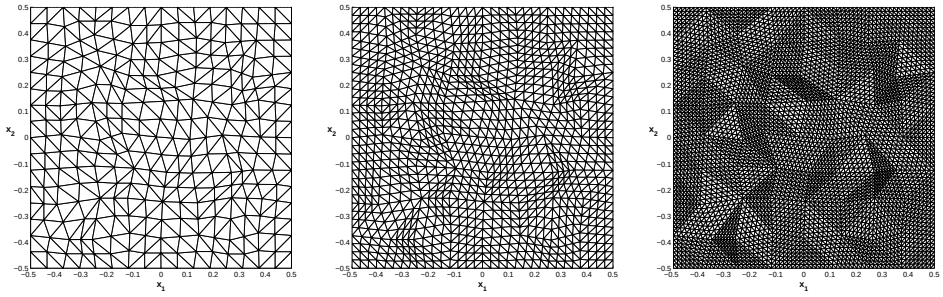

$\mathbf{A}_1$ ($h = 1/16$) $\mathbf{A}_2$ ($h = 1/32$) $\mathbf{A}_3$ ($h = 1/64$)

FIGURE 1. Mesh sequence $\mathbf{A}_1$–$\mathbf{A}_3$ and their mesh widths h.

Following [7, 15], we let $\rho = 4$ and $\epsilon = 10^{-5}$ in (13) for the construction of the WENO weights ω_i. Our numerical results are reflected by Table 2, where the resulting approximation error and the corresponding convergence rates

$$E_p(h) = \|u_h - \tilde{u}\|_p \text{ and } k_p = \frac{\log[E_p(h)/E_p(h/2)]}{\log(2)}, \qquad \text{for } p = 1, 2, \infty,$$

are shown for the norms $\|\cdot\|_1$, $\|\cdot\|_2$, and $\|\cdot\|_\infty$.

Note that the proposed WENO reconstruction attains, in combination with the fourth order Lax-Friedrichs flux approximation (4) and the third order TVD-RK method (6) convergence rates of up to order four, which

TABLE 2. WENO reconstruction by thin plate splines. Approximation errors and corresponding convergence rates.

h	$E_1(h)$	k_1	$E_2(h)$	k_2	$E_\infty(h)$	k_∞
1/16	$1.8417 \cdot 10^{-5}$	–	$1.1968 \cdot 10^{-4}$	–	$9.6658 \cdot 10^{-4}$	–
1/32	$4.1100 \cdot 10^{-6}$	4.12	$6.8725 \cdot 10^{-6}$	4.12	$6.8089 \cdot 10^{-5}$	3.82
1/64	$2.5679 \cdot 10^{-7}$	4.00	$5.5042 \cdot 10^{-7}$	3.64	$8.4387 \cdot 10^{-6}$	2.69

exceeds the expected order $k = 2$ of the thin plate spline reconstruction scheme. But our numerical results are consistent with earlier numerical observations concerning bivariate interpolation from periodic input data over regular grids. Moreover, the obtained results comply with theoretical results in [3, 4, 21] where higher order convergence is proven for thin plate spline interpolation from sufficiently smooth bivariate target functions. For details on the analysis and the different underlying assumptions on the target function, we refer to [3, 4, 21] and [27, Section 11].

Let us finally remark that our obtained convergence rates are comparable to those in [15] obtained by fourth order ADER finite volume methods (for the norms $\|\cdot\|_1$, $\|\cdot\|_2$) and third order ADER finite volume methods (for the norm $\|\cdot\|_\infty$), each relying on polynomial WENO reconstructions of order four and three, respectively. For a detailed documentation, see the numerical results in [15].

6. Conclusion

Polyharmonic splines are applied in WENO reconstruction to obtain high order finite volume methods. Unlike traditional WENO schemes, where polynomial reconstructions are used, polyharmonic spline WENO reconstructions

- are numerically stable;
- allow for flexible stencil constructions;
- yield optimal reconstructions in associated Beppo Levi spaces;
- provide natural choices for the oscillation indicator $\mathcal{I}$.

Moreover, polyharmonic spline reconstruction is, like polynomial reconstruction, of arbitrary high local approximation order, see Subsection 3.4.

Acknowledgement

The first author is supported by a Commonwealth Scholarship, references NGCA-2004-55.

References

[1] R. Abgrall, On ENO schemes on unstructured meshes: analysis and implementation. J. Comput. Phys. **114**(1994), 45–58.

[2] R. Artebrant and H.J. Schroll, *Limiter-Free Third Order Logarithmic Reconstruction*. Technical Report, University of Lund, 2004.

[3] A. Bejancu, Local accuracy for radial basis function interpolation on finite uniform grids. J. Approx. Theory **99**(1999), 242–257.

[4] M.D. Buhmann, *Multivariable Interpolation Using Radial Basis Functions*. Ph.D. thesis, University of Cambridge, 1989.

[5] M.D. Buhmann, *Radial Basis Functions*, Cambridge University Press, 2003.

[6] J. Duchon, Splines minimizing rotation-invariant semi-norms in Sobolev spaces. In: *Constructive Theory of Functions of Several Variables*, W. Schempp and K. Zeller (eds.), Springer, Berlin, 1977, 85–100.

[7] O. Friedrich, Weighted essentially non-oscillatory schemes for the interpolation of mean values on unstructured grids. J. Comput. Phys. **144**(1998), 194–212.

[8] A. Harten and S.R. Chakravarthy, *Multidimensional ENO Schemes for General Geometries*. ICASE Report **91-76**, 1991.

[9] A. Harten, B. Engquist, S. Osher, and S.R. Chakravarthy, Uniformly high order accurate essentially non-oscillatory schemes III. J. Comput. Phys. **71**(1987), 231–303.

[10] C. Hu and C.W. Shu, Weighted essentially non-oscillatory schemes on triangular meshes. J. Comput. Phys. **150**(1999), 97–127.

[11] A. Iske and T. Sonar, On the structure of function spaces of optimal recovery of point functions for ENO schemes by radial basis functions. Numerische Mathematik **74**(1996), 177–201.

[12] A. Iske, On the approximation order and numerical stability of local Lagrange interpolation by polyharmonic splines. In: *Modern Developments in Multivariate Approximation*, W. Haussmann, K. Jetter, M. Reimer, and J. Stöckler (eds.), International Series of Numerical Mathematics **145**, 2003, Birkhäuser, Basel, 153–165.

[13] A. Iske, *Multiresolution Methods in Scattered Data Modelling*. Springer, Berlin, 2004.

[14] G.S. Jiang and C.W. Shu, Efficient implementation of weighted ENO schemes. J. Comput. Phys. **126**(1996), 202–228.

[15] M. Käser and A. Iske, ADER schemes on adaptive triangular meshes for scalar conservation laws. J. Comput. Phys. **205**(2005), 486–558.

[16] R.J. LeVeque, *Finite Volume Methods for Hyperbolic Problems*. Cambridge University Press, 2002.

[17] X.D. Liu, S. Osher, and T. Chan, Weighted essentially non-oscillatory schemes. J. Comput. Phys. **115**(1994), 200–212.

[18] C.A. Micchelli, Interpolation of scattered data: distance matrices and conditionally positive definite functions. Constr. Approx. **2**, 1986, 11–22.

[19] C.A. Micchelli and T.J. Rivlin, A survey of optimal recovery. In: *Optimal Estimation in Approximation Theory*, C.A. Micchelli and T.J. Rivlin (eds.), Plenum, New York, 1977, 1–54.

[20] F.J. Narcowich and J.D. Ward, Norm estimates for the inverses of a general class of scattered-data radial-function interpolation matrices. J. Approx. Theory **69**, 1992, 84–109.

[21] R. Schaback, Improved error bounds for scattered data interpolation by radial basis functions. Math. Comp. **68**(1999), 201–216.
[22] C.W. Shu, Total-variation-diminishing time discretizations. SIAM J. Sci. Stat. Comput. **9**(1988), 1073–1084.
[23] C.W. Shu and S. Osher, Efficient implementation of essentially non-oscillatory shock capturing schemes. J. Comput. Phys. **77**(1988), 439–471.
[24] T. Sonar, Optimal recovery using thin plate splines in finite volume methods for the numerical solution of hyperbolic conservation laws. IMA Journal of Numerical Analysis **16**(1996), 549–581.
[25] T. Sonar, On the construction of essentially non-oscillatory finite volume approximations to hyperbolic conservation laws on general triangulations: polynomial recovery, accuracy and stencil selection. Computer Methods in Applied Mechanics and Engineering **140**(1997), 157–181.
[26] T. Sonar, On families of pointwise optimal finite volume ENO approximations. SIAM Journal of Numerical Analysis **35**(1998), 2350–2369.
[27] H. Wendland, *Scattered Data Approximation*, Cambridge University Press, 2005.
[28] Z. Tang, A new approach to construct WENO schemes. Paper presented at Aerospace Science Meeting and Exhibit, Jan. 8-11, 2001.
[29] V.A. Titarev and E.F. Toro, ADER: Arbitrary high order Godunov approach. J. Sci. Comput. **17**(2002), 609–618.
[30] E.F. Toro. *Riemann Solvers and Numerical Methods for Fluid Dynamics*. Springer, 2nd edition, 1999.

Terhemen Aboiyar, Department of Mathematics, University of Leicester, Leicester, LE1 7RH, United Kingdom
E-mail address: ta57@le.ac.uk

Emmanuil H. Georgoulis, Department of Mathematics, University of Leicester, Leicester, LE1 7RH, United Kingdom
E-mail address: Emmanuil.Georgoulis@mcs.le.ac.uk

Armin Iske, Department of Mathematics, University of Hamburg, D-20146 Hamburg, Germany
E-mail address: iske@math.uni-hamburg.de